A SAMPLING METHOD FOR INVESTIGATING SELF-HEALING PROPERTY OF CONCRETE DAMAGED BY THE DRYING SHRINKAGE

Hoang Vinh Long[1]*

Abstract: *This paper briefly overviews experimental procedure and methods of self-healing studies; and the damage of concrete materials due to drying shrinkage. Microstructure observations such as SEM, ESEM are used as popular methods in self-healing researches; however, they are difficult to be carried out in case of 3D-cracks.To solve the problem, this study proposes a sampling method that makes easier to be observe the microstructure of products on surfaces of simulated cracks.*

Keywords: *self-healing, drying shrinkage, SEM.*

Received: October 5th, 2017; revised: October 31th, 2017; accepted: November 2nd, 2017

1. Introduction

Self-healing is an interesting behavior of cementitious materials in which the materials could heal their own damages automatically. This behavior has been observed for over hundred years [1,2], and obtained much more scientist's attention for the last several decades. During the self-healing process, cracks could be filled and bridged by new products. These products are produced based on many mechanisms such as continuous hydration, carbonation, dissolution and deposition of $Ca(OH)_2$ [1,3]. Furthermore, cracks may be closed by dilatation of hydrated products that also contributes to the self-healing. As a result, the damaged materials could recover strength and reduce permeability due to self-healing ability.

Many methodologies have been used to investigate the self-healing property of concrete. Brief overview of the methods and damage by drying conditions are presented in this paper.

1.1 Experimental procedures and research methods - An overview

Various methods are used in self-healing researches. Generally, experimental procedures are shown in Fig. 1, and research methods are given in Table 1.

Mostly inducing damages is an obligatory step in procedures of self-healing researches, and methods are usually based on standard tests, such as the rapid free/thaw cycles based on ASTM C666 were used to crack specimens in many researches [4-6]. Modified strength tests are another way to crack specimen, for example: pre-loaded up to 70% and 90% of compressive load determined at 28 days to generate cracks [7]; variable compressive load to pre-crack [8]; pre-cracked specimens by tensile load up to 3% tensile strain [9]. Other scientists [3,10] conducted bending test and controlled crack width by CMOD sensor. In a research at Delf University of Technology [11], they also used a three-point bending test, and set up a compressive load to close a part of crack later on. A splitting test is often used in self-healing research, such as in works [12,13]. It is a similar idea that a non-standard test with a cutting force was set up [14]. By another approach, micro-cracks generated by autogenous shrinkage and a self-healing process in pores was investigated [15]. Moreover, simulated a crack by using a thin plate of 0.3 mm was also in a self-healing research [16].

A number of techniques are used to detect and/or quantify self-healing ability of cementitious materials. As shown in the procedures in Fig. 1, several tests are usually conducted before cracking (test 1),

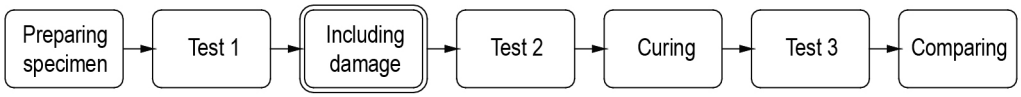

Figure 1. *Typical experimental procedure of a self-healing research*

[1] Dr, Faculty of Building Materials, National University of Civil Engineering.
** Corresponding author. E-mail: longhv@nuce.edu.vn.*

after cracking (i.e. before healing-test 2) and after curing (i.e. after healing-test 3). The comparison between test-1 results and test-2 results of the same type of techniques often presents damage degree. Similarly, the comparison between test-2 results and test-3 results give the self-healing capability of material. Among the techniques, mechanical tests and permeability tests are considered more direct methods to quantify self-healing capability. SEM observation is often used to explain mechanism of a self-healing process (see Fig. 2). According to [17], although the acoustic emission analysis and UPV measurement can detect the occurrence of the crack healing, they cannot accurately determine the extent of the crack healing.

Table 1. *Typical methods used in self-healing researches*

	Methods
Damage generation	Tensile load: uniaxial, splitting Bending load: three-point, four-point bending test Compressive load Rapid freeze/thaw Very thin plate Autogenous shrinkage
Curing conditions	Curing environment: Water (submerged) Lime saturated water Water-dry cycles Chloride solution submersion High humidity Natural weather Air in the laboratory Curing time: normally 1 month to 12 months Temperature: normally lower than 80°C
Self-healing investigations	Mechanical tests: compressive, tensile, flexural test Water permeability test Chloride migration Ultrasonic Pulse Velocity (UPV) Resonant Frequency Acoustic emission analysis Microscopic observation and analysis: SEM, XEDS Porosity

Controlling crack width and detecting new products on crack surfaces are important issues when cracking methods are choosen. Using a tensile load, a flexural load and a splitting load can be suitable to control the position of crack, but they do not control crack width well. Rapid free/thaw cycles, a compressive load, autogenous shrinkage and drying shringkage generate 3D-cracks in a specimen. Therefore, it is difficult to control crack position, crack width, and especially to observe new products on crack space when these methods are chosen.

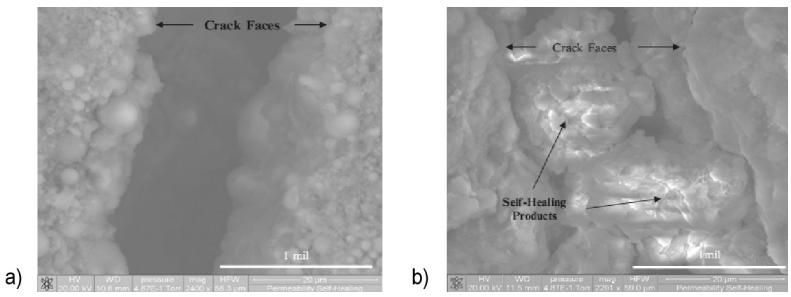

Figure 2. *Observation by ESEM is a common method of self-healing research (a) Crack before self-healing; (b) Autogenous crystalline formations after self-healing [17]*

1.2 Damage by drying conditions

1.2.1 Introduction to drying shrinkage

Besides an external load, shrinkages are an important reason causing deformation of cementitious materials as exposed to an environment. Shrinkages of cementitious materials are divided into several

categories: thermal shrinkage, drying shrinkage, autogenous shrinkage, plastic shrinkage and carbonation shrinkage [18,19]. Microstrain of drying shrinkage, 400 to 1000×10^{-6}, is quite large and cannot be ignored in large-dimensional concrete structures. Additionally, concrete structures are commonly damaged by drying shrinkage. Therefore, many works have focused on studying an area of drying shrinkage.

Drying shrinkage is defined as the time-dependent volume change induced by water loss in a specimen which is allowed to be dried by being exposed to an environment with certain relative humidity and temperature [18].

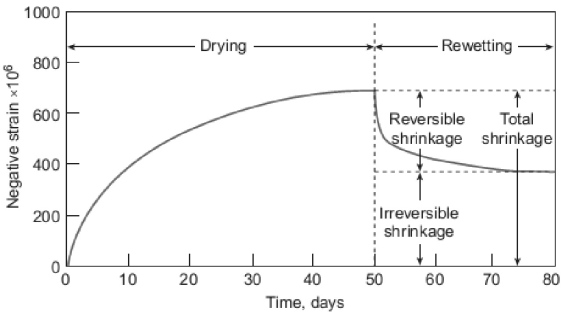

Figure 3. *Reversibility of drying shrinkage [20]*

A porous structure is a characteristic of cementitious materials with a minimum porosity of some 28% of a paste specimen. For workability purpose, the amount of water added to a mixture is usually higher than the requirement for reactions. Therefore, the porosity is practically in order of 50%. Consequently, water content containing in the porous structure varies due to moisture exchange with environment that results in volume change of cementitious materials. An increase in moisture content causes a volume increase (i.e. swelling). In contract, moisture migration due to low relative environment is the driving force for volume reduction. In practice, the shrinkage plays a more important role than the swelling on performance and durability of concrete.

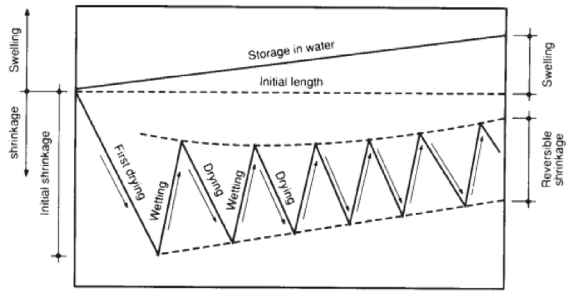

Figure 4. *Schematic description of volume changes in concrete exposed to alternate cycles of drying and wetting [21]*

A notable phenomenon is irreversible shrinkage when cementitious materials are subjected to a cycle of drying and wetting. The shrinkage in drying phase is reversed but usually in a smaller amount. Schematics describing this phenomenon are shown in Figs. 3 and 4. It is proposed that the irreversible drying shrinkage is probably due to new bonds within the C-S-H sheets as a consequence of drying [19,20].

1.2.2 Damage due to drying condition in cementitious materials

a) Induced microcracks on drying process

In cement-based materials, two main types of internal restraint usually occur: self-restraint and aggregate restraint, they are considered to be the reason of drying shrinkage microcracks. In this study, paste specimen will be damaged by the drying condition, so only a self-restraint is concerned.

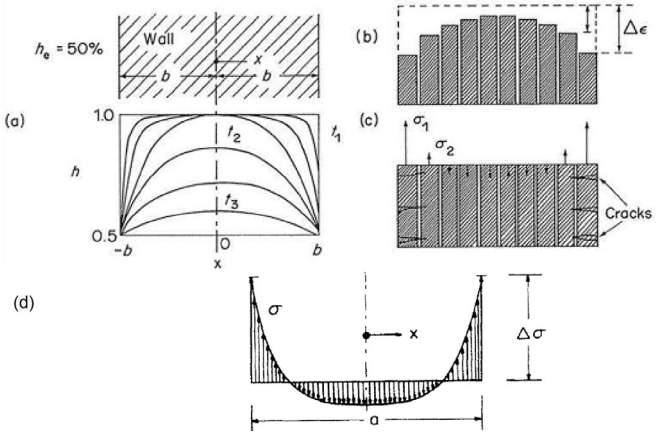

Figure 5. *A concrete wall exposed to drying: (a) Geometry and RH distribution at different drying times; (b) corresponding shrinkage strains for each layer, as if they were not subjected to any kind of restriction; (c) induced-stresses and cracking due to restoration of compatibility conditions [22]; (d) a typical distribution of shrinkage stresses throughout a wall [23]*

The driving force of self-restraint is non-uniform shrinkage of a specimen as a result of the moisture gradient that develops upon drying (see Figs.5 a, b). As a result, the non-uniform shrinkage inevitably leads to stress. The stress-distribution in a drying wall was calculated as Fig. 5d [23]. At the beginning of drying the largest shrinkage stresses are produced near the drying surface, and compressive stress is occurred in the core of the wall. The self-restraint leads to crack if the maximum tensile stress (σ_{max}) exceeds the tensile strength of cementitious paste. Microcracks will mainly develop perpendicular to the drying surface. It [23] was also estimated the maximum admissible moisture gradient (i.e., drying rate) and maximum wall thickness to avoid microcracks.

In terms of fracture mechanics, cementitious paste is considered homogeneous. On the microscopic scale, however, the modulus of elasticity between hydrated cement and clinker residue or admixture particles are different. Therefore, the heterogeneity of the paste could result in stresses high enough to cause microcracks in matrix [24].

In cement-base paste, drying shrinkage crack is considered as microcracks due to its very small crack-width. A RILEM state-of-the-art report on microcracking suggested that this limit could be 10 μm [25]. However, it was claimed [26,27] that the term microcrack should be used for cracks with a width smaller to 50 μm, which is typically the maximum crack opening for the drying shrinkage induced cracks. Moreover, the experiment [28] was conducted with cement paste with W/C=0.35, 0.45 and 0.6 and temperature treatment at 40°C, 80°C and 105°C to generate cracking network. By using an optical microscope, he measured crack width at ranges 50 to 100 μm.

b) Superficies of paste cracks and modeling

Commonly, a surface-crack pattern shows polygonal shapes, so that larger crack spacing would correspond to larger polygons, as shown in Fig. 6. Spacing of crack varies in the large range from 10 to 90 mm normally. The depth of micro-cracks parallel to drying surfaces is typically between 3 and 6 mm [26]. It was reported the mean crack spacing Lm was about 10 to 15 mm [28].

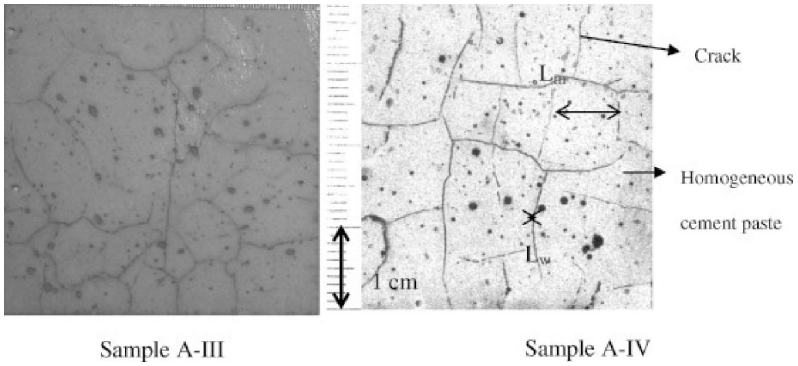

Figure 6. *Crack network of cement paste specimens with W/C=0.35 in which samples A-III and A-IV exposed to 80°C and 105°C respectively [28]*

2. A proposal of a sampling method

As mentioned in Section 1, the microstructure observation is a popular method in self-healing researches. However, cracks generated by drying shrinkage appeared in a 3D pattern; therefore, observing new products in such cracks' space to understand a healing process is difficult. This study proposes a sampling method to make the observation easier in which simulated cracks was created by cutting then grafting specimens as shown in Fig. 7.

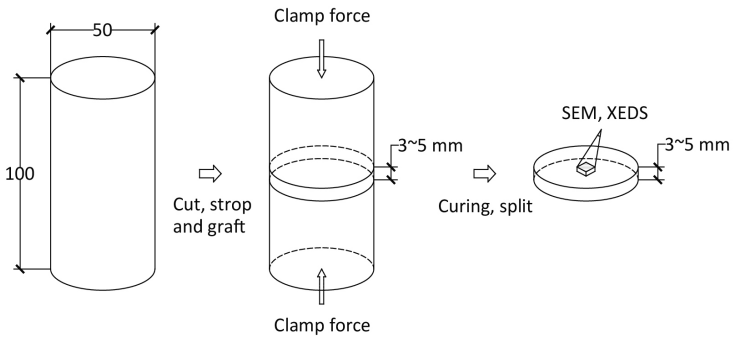

Figure 7. *Prepared procedure of SEM and XEDS observations*

After being dried in a oven for seven days, specimen was cut into three parts. Next, the surfaces of each part were stropped until flat. The middle slice was 3-5 mm thick, which is easy to use in SEM observation. After that the three parts were kept together by a clamp. Then all of specimens with the clamp were put in a curing condition. By the observation time, the sample is split up manually and the middle to conduct into SEM and XEDS test conduction.

3. Materials and methods

3.1 Materials

The materials used in this study were Type-I Portland cement, class F fly ash and crystalline additive Xypex Admix C-2000. The cement following ASTM C150 was provided by Taiwan Cement Corporation. The fly ash was from Taiwan Power Company following ASTM C618. Chemical compositions of cement and fly ash were given in Table 2. Xypex Admix C-2000 from Xypex Chemical Corporation comprises Portland cement, very fine treated silica sand and various active proprietary chemicals.

Table 2. *Chemical composition of cement and fly ash*

	SiO_2	Al_2O_3	Fe_2O_3	SO_3	Na_2O	K_2O	CaO	MgO	LOI
Cement	21.04	6.24	3.06	3.22	-	-	63.86	1.54	1.04
Fly ash	50.00	28.41	6.98	0.47	0.09	0.13	5.99	1.39	4.62

3.2 Methods

To compare the difference in microstructure between on surface of simulated cracks and inside of specimens, the test procedures of the present study was set up as in Fig. 8. After being removed from molds, specimens with diameter × length = 50×100 mm were cured in lime-saturated water at room temperature 25±2°C for six days. Next, group-I specimens were continuously cured in the same environment. Then group-I specimens were conducted SEM and XEDS tests with sample split from inside of specimens. To generate cracks, group-II specimens were dried in an oven at 50±1°C for seven days. This drying condition was severe compared to natural drying, but was chosen due to expectation to lead more microcracks. After being cut, stropped and grafted as described in Fig. 7, group-II specimens were cured and conducted in the microscope observation with a sample split from the surface of slides at the same day.

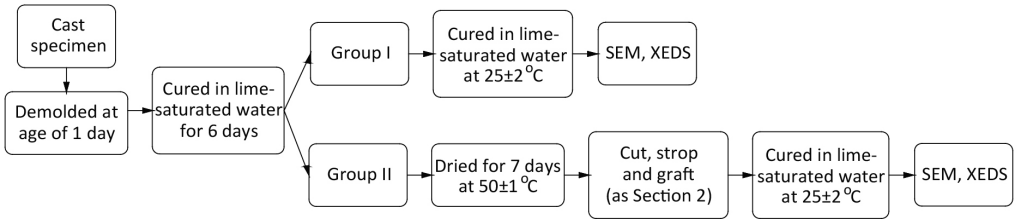

Figure 8. *Experiment procedure*

4. Test results

This study only addresses to the drying shrinkage and expects to neglect autogenous shrinkage. It has been reported that if W/C ratio high enough autogenous is insignificant. For example, it was claimed [29] that if a paste has a W/C ratio higher than 0.4 and is cured in water for six days after one-day molding, then the influence of autogenous shrinkage on the paste's microstructure could be negligible. Therefore, as shown in Table 3, two mixes containing cement, fly ash, xypex, and water were used in this study; and W/B was kept constant at 0.42 by weight. M1 specimens contained the Portland cement. In mixes M2, pastes consisted cement, fly ash and xypex in which fly ash replacement at rate of 45%, and xypex was used at rate of 2% by weight of binder.

Table 3. *Mix design of pastes by weight ratio (%)*

Mix	Description	Cement	Fly ash	Xypex	Water
M1	PC	100	0	-	42
M2	FC45-XP	55	45	2	42

After preparation as shown in Fig. 8, specimens of group I and group II were conducted in SEM and XEDS tests. As given in Figs.9 and 10, results of SEM observations are shown clearly the change morphology of products on specimen surfaces comparing to the inside of specimen.

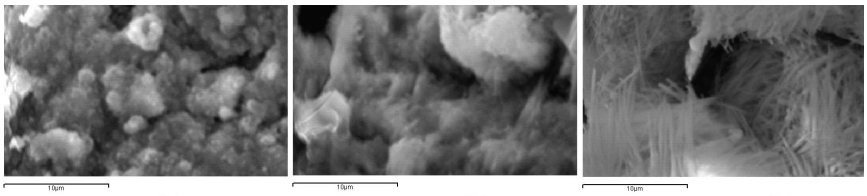

(a) (b) (c)

Figure 9. *SEM observations of M1(PC) specimens: (a) group-I, at age of 14 days; (b) group-I, at age of 120 days; (c) group-II, on slice surface at age of 120 days*

The microstructure morphology of Portland cement paste (M1) was studied by SEM (see Fig. 9). At age of 14 days, C-S-H clusters occupied, they were quite uniform at about 3 μm in size. The microstructure of group-I much improved at the age of 120 days with well connections and bigger flattened particles. Interestingly, new products occurring on slice surface (see Fig. 9c) were fibrous particles which were significantly different from that of group-I in Fig. 9b. The Ca:Si:Al:S ratios of group-I were 1:0.27:0.07:0.04.The ratios of the new products were 1:0:0.3:0.42 of case (c) in Fig. 9 which was approximately the AFt composition. According to [30], high temperature of drying environment at early and additional penetrating $Ca(OH)_2$ may be the reason of delay AFt formation that occurred on the slide surface.

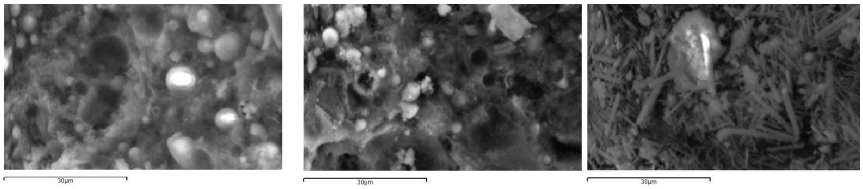

(a) (b) (c)

Figure 10. *SEM observations of M2 (FC45-XP) specimens: (a) group-I, at age of 14 days; (b) group-I, at age of 91 days; (c) group-II, on slice surface at age of 91 days*

As shown in Figure 10(a) and (b), fly ash particles were smaller and much sunk in matrix at the age of 91 days than they were done at age of 14 days. It may be explained that the addition alkaline amount provided by xypex could accelerate breaking of fly ash glass. Consequently, it speeded up reactions in cement-fly ash-xypex system. When comparing Figs. 10 (b) and (c), the different products were obviously observed in two cases of M2 specimens. The needle-like particles occurred clearly on the slice surface (see Fig. 10c). The ratio Ca:Si:Al: =1:0.27:0.21:0.18 determined on the such surface is closed to AFm composition, excluding Si element.

5. Conclusions

This study proposes a sampling method that make easier to observe microstructure on surfaces of simulated crack. By this method, the differences of products between inside specimens and on surface of simulate cracks were clearly observed on two group specimens. The test results suggest that the method could be used suitably to investigate the self-healing property in case of 3D-cracksdue to external factors such as a drying environment.

References

1. Hearn N.(1998), "Self-sealing, autogenous healing and continued hydration: What is the difference?", *Materials and Structures/Materiaux et Constructions*, 31:563-567.

2. Qian S., Zhou J., Rooij M.R.D., Schlangen E., Ye G., Van B.K. (2009), "Self-healing behavior of strain hardening cementitious composites incorporating local waste materials", *Cement and Concrete Composites*, 31:613-621.

3. Granger S., Pijaudier C.G., Loukili A, Marlot D., Lenain J.C. (2009), "Monitoring of cracking and healing in an ultra high performance cementitious material using the time reversal technique", *Cement and Concrete Research*, 39:296-302.

4. Jacobsen S., Marchand J., Boisvert L. (1996), "Effect of cracking and healing on chloride transport in OPC concrete", *Cement and Concrete Research*, 26:869-881.

5. Jacobsen S., Marchand J., Hornain H. (1995), "SEM observations of the microstructure of frost deteriorated and self-healed concretes", *Cement and Concrete Research*, 25:1781-1790.

6. Jacobsen S., Sellevold E.J. (1996), "Self healing of high strength concrete after deterioration by freeze/thaw", *Cement and Concrete Research*, 26:55-62.

7. Şahmaran M., Keskin S.B., Ozerkan G., Yaman I.O. (2008), "Self-healing of mechanically-loaded self consolidating concretes with high volumes of fly ash", *Cement and Concrete Composites*, 30:872-879.

8. Zhong W. , Yao W. (2008), "Influence of damage degree on self-healing of concrete", *Construction and Building Materials*, 22:1137-1142.

9. Yang Y., Lepech M.D.,Yang E.H., Li V.C. (2009), "Autogenous healing of engineered cementitious composites under wet-dry cycles", *Cement and Concrete Research*, 39:382-390.

10. Granger S., Loukili A., Pijaudier C.G., Chanvillard G. (2007), "Experimental characterization of the self-healing of cracks in an ultra high performance cementitious material: Mechanical tests and acoustic emission analysis", *Cement and Concrete Research*, 37:519-527.

11. Ghosh S.K. (2009), *Self-healing Materials: Fundamentals, design strategies, and applications.*: John Wiley & Sons.

12. Reinhardt H.W., Jooss M. (2003), "Permeability and self-healing of cracked concrete as a function of temperature and crack width", *Cement and Concrete Research*, 33: 981-985.

13. Sisomphon K., Copuroglu O., Koenders E.A.B (2012), "Self-healing of surface cracks in mortars with expansive additive and crystalline additive", *Cement and Concrete Composites*, 34:566-574.

14. Li V.C., Lim Y.M., Chan Y.W (1998), "Feasibility study of a passive smart self-healing cementitious composite", *Composites Part B: Engineering*, 29:819-827.

15. Termkhajornkit P., Nawa T., Yamashiro Y., Saito T.(2009), "Self-healing ability of fly ash-cement systems", *Cement and Concrete Composites*, 31:195-203.

16. Tittelboom K.V, De Belie N., De Muynck W., Verstraete W.(2010), "Use of bacteria to repair cracks in concrete", *Cement and Concrete Research*, 40:157-166.

17. Li V.C, Yang E.H (2007), Self Healing in Concrete Materials in *Self Healing Materials - An Alternative Approach to 20 Centuries of Materials Science, S. Zwaag*, Ed., ed: Springer Netherlands, 100:161-193.

18. ACI (2005), 209.1R-05: *Report on Factors Affecting Shrinkage and Creep of Hardened Concrete*.

19. Mehta P.K., Monteiro P.J.M (2006), *Concrete: microstructure, properties, and materials*: McGraw-Hill.

20. Mindess S., Young J.F., Darwin D. (2003), *Concrete*: Prentice Hall.

21. Soroka I. (1993), *Concrete in Hot Environments*: E&FN Spon.

22. Bazant Z.P. (1988), *Mathematical model of creep and shrinkage of concrete*: John Wiley & Sons Ltd.

23. Baănt Z.P., Raftshol W.J. (1982), "Effect of cracking in drying and shrinkage specimens", *Cement and Concrete Research*, 12:209-226.

24. Hearn N. (1999), "Effect of Shrinkage and Load-Induced Cracking on Water Permeability of Concrete", *ACI Materials Journal*, 96:234-241.

25. Jensen A.D., Chatterji S. (1996), "State of the art report on micro-cracking and lifetime of concrete-Part 1", *Materials and Structures*, 29:3-8.

26. Bisschop J. (2002), *Drying shrinkage microcracking in cement-based materials*, Ph.D., Delft University of Technology, The Netherlands.

27. Shiotani T., Bisschop J., Mier J.G.M.V. (2003), "Temporal and spatial development of drying shrinkage cracking in cement-based materials", *Engineering Fracture Mechanics*, 70:1509-1525.

28. Caré S. (2008), "Effect of temperature on porosity and on chloride diffusion in cement pastes", *Construction and Building Materials*, 22:1560-1573.

29. Tazawa E., Miyazawa S. (1997), "Influence of constituents and composition on autogenous shrinkage of cementitious materials", *Magazine of Concrete Research*, 49:15-22.

30. Taylor H.F.W, Famy C., Scrivener K.L. (2001), "Delayed ettringite formation", *Cement and Concrete Research*, 31:683-693.